

X-Ray Sources in Regions of Star Formation.
VI. The R CrA Association as Viewed by *EINSTEIN*.

Frederick M. Walter^{1,2}

Department of Physics and Astronomy, State University of New York, Stony Brook NY
11794-3800

I:fwalter@astro.sunysb.edu

Frederick J. Vrba²

U.S. Naval Observatory, Flagstaff Station, Flagstaff AZ 86002

I:fjv@nofs.navy.mil

Scott J. Wolk²

Earth and Space Sciences Department, State University of New York, Stony Brook NY
11794-2100 and Harvard-Smithsonian Center for Astrophysics, Cambridge MA 02138

I:swolk@head-cfa.harvard.edu

Robert D. Mathieu

Department of Astronomy, University of Wisconsin, Madison WI 53706 and
Harvard-Smithsonian Center for Astrophysics, Cambridge MA 02138

I:mathieu@astro.wisc.edu

Ralph Neuhäuser

Max-Planck-Institut für Extraterrestrische Physik, 85740 Garching, Germany

I:rne@hpth03.mpe-garching.mpg.de

ABSTRACT

We report on optical identifications of X-ray sources in the vicinity of the R CrA association. We identify 11 low-mass pre-main-sequence stars as counterparts of 9 X-ray sources. We also find X-ray emission from coordinates consistent with the position of 3 bright late-B stars, although the emission may come from lower mass companions. The X-ray-selected stars lie along a

¹Guest Observer, EINSTEIN Observatory.

²Visiting Astronomer, Cerro Tololo Inter-American and Kitt Peak National Observatories, National Optical Astronomy Observatories, which are operated by the Association of Universities for Research in Astronomy, Inc., under contract with the National Science Foundation.

narrow locus in the luminosity-temperature diagram at an age of about 7 Myr, which is considerably older than the estimated ages of the higher mass stars or of the IR-excess stars. We determine the physical characteristics of these stars, including masses, ages, and Lithium abundances. We estimate that the complete membership of the R CrA association amounts to about 90 stars, mostly older naked T Tauri stars, and that the population is consistent with the standard IMF.

1. Introduction

The R CrA association, at a distance of about 130 pc (Marraco & Rydgren 1981), is one of the nearest star-forming associations to the Sun. The association is projected against a prominent dark cloud 18° below the galactic plane (see figure 1 of Knacke *et al.* 1973). The total mass of the cloud is estimated to be between 3000 and 10,000 M_\odot (Dame *et al.* 1987; Loren 1979). Wilking *et al.* (1994) comment that the morphology of the cloud bears a resemblance to the ρ Oph cloud. However, the number of known and suspected members of the stellar association is only 10% of that known or suspected in ρ Oph.

Knacke *et al.* (1973) discovered a group of 11 young stars near R CrA. Members of the association include the intermediate-mass stars R, T, and TY CrA and the classical T Tauri stars S, VV, and DG CrA. Nine of the 11 stars had near-IR continuum excesses. Knacke *et al.* also identified 10 $H\alpha$ -emitting stars spread over the region, at projected distances up to a half degree from the dark cloud. Glass & Penston (1975) undertook near-IR photometry of 44 stars in this region, and noted that the only stars with near-IR continuum excesses were the known variable stars. They failed to detect near-IR excesses for 3 of the $H\alpha$ -emitting stars identified by Knacke *et al.*, and commented that $H\alpha$ emission and $2\mu\text{m}$ excesses do not necessarily correlate. Marraco & Rydgren (1981) reexamined the association. They found $H\alpha$ emission in only 4 of the 10 Knacke *et al.* sources, but discovered another 6 $H\alpha$ -emitting objects. Wilking *et al.* (1992) surveyed this region using the IRAS data, finding 16 IRAS sources associated with young stellar objects (YSOs). They identified 24 YSOs from their near- and far-IR spectral energy distributions. Wilking *et al.* (1994) presented results of near-IR imaging of the cloud core, and concluded that there are approximately 30 members of this association.

Knacke *et al.* (1973) estimated an association age of less than 10^6 years (1 Myr), assuming that the late-B stars of the association have just arrived on the main-sequence. Wilking *et al.* (1992) estimate an age of between 1.5 Myr (the contraction age of the zero-age main sequence B8 star TY CrA) and 6 Myr (the contraction time for the pre-main

sequence A5 star R CrA).

While infrared observations can be useful in identifying low-mass pre-main-sequence (PMS) stars, experience over the past decade has shown that the population sampled in the infrared is not necessarily representative of the true population of young associations. X-ray imaging observations (e.g., Feigelson & Kriss 1981; Montmerle *et al.* 1983; Feigelson *et al.* 1993; Mundt *et al.* 1983; Strom & Strom 1994; Walter *et al.* 1988, 1994) of young associations reveal a population of X-ray-luminous young stars which generally lack infrared continuum excesses. Walter (1986) found 3 X-ray-luminous PMS stars near the CrA cloud. Here we report on the complete EINSTEIN Observatory Imaging Proportional Counter (IPC) observations of the CrA dark cloud. In addition to the 3 sources previously identified, there are another 8 X-ray sources. In this paper we discuss the identifications of these X-ray sources.

2. Observations

2.1. X-Ray Observations

The X-ray data consist of the two overlapping IPC observations listed in Table 1 and shown in Figure 1. The IPC ribs, which support the detector window, obscure $\sim 30\%$ of the nominal 1 square-degree field of the IPC. There is significant vignetting in the IPC; effective exposure times at the edge of the field (30 arcmin from the center) are about 50% of those on-axis.

The IPC is sensitive to photons with energies between about 0.1 and 4.5 keV. Active stellar coronae have characteristic temperatures of 10^7K , or about 1 keV, and are well matched to the IPC response. The energy resolution of the IPC is about 100%, and only gross spectral information is available for weak sources. The 90% confidence uncertainty on the X-ray source positions is typically $\pm 30\text{-}40$ arcseconds. Details of the IPC are given in Giacconi *et al.* (1979).

There are three X-ray sources in IPC sequence 3501, centered on ϵ CrA (HD175813). Two of these were found in the standard rev 1B processing of sequence. The MDETECT (map detect) source detection algorithm had not run as a part of the standard processing. We requested that MDETECT be run off-line, and it yielded the third X-ray source. In IPC sequence 4512, centered on the CrA dark cloud, the standard processing yielded 10 X-ray sources.

2.2. Optical and near-IR observations

All of the X-ray sources had potential optical counterparts on the POSS sky survey. The W UMa star ϵ CrA (Cruddace & Dupree 1984) was detected in both IPC observations. The other X-ray sources, their J2000 coordinates, and aliases, are presented in Table 2.

We obtained low-dispersion spectra of these stars at the Kitt Peak National Observatory in June 1983, April 1986, and May 1987, using the Intensified Image Dissector Scanner (IIDS) on the 2.1-m telescope. All observations were made through the 7-arcsecond aperture. Observations in the red covered the range 6150-7200Å at about 3Å resolution, and were obtained with grating 36 and the GG495 order-sorting filter. Blue observations, taken using grating 36 and the CuSO₄ order-sorting filter, covered the range 3750-4200Å with about 1.5Å resolution. The spectra were fully reduced and wavelength- and flux-calibrated using the mountain data reductions and the IPPS software package. Flux calibration relied on the IRS standard stars (Barnes & Hayes 1982). Subsequent data analysis was performed using software written in IDL.

Low-dispersion spectra were also taken on 18 and 23 July 1995, and on 21 July 1996, at the European Southern Observatory (ESO) using the 1.52m telescope equipped with a Boller and Chivens spectrograph. We used grating #5 and CCD #24 (in 1995) or CCD #39 (in 1996), achieving a mean resolution of about 2.5Å (FWHM) in the 4600-7000Å spectral range. This instrumental set-up allows us to resolve the Lithium I absorption line at 6707Å from the Ca I absorption line at 6717Å as well as to carry out an accurate spectral type classification. For the wavelength calibration, a He-Ar exposure was taken after each science exposure. The standard stars LTT 4816, LTT 7987, and EG 274 were observed each night with the same instrumental set-up to perform the flux calibration. We used the MIDAS software (versions 95MAY and 95NOV) to reduce these spectra. Bias and dark subtraction was first performed on each frame. The 2-D science frames were then divided by a mean flat-field and then calibrated in wavelength. The sky subtraction, the extraction of one dimensional spectra and the flux calibration using a mean response function, were finally performed.

High-dispersion spectra were obtained using the Cerro Tololo Inter-American Observatory (CTIO) 4-m echelle on 4-6 April 1987 and 23-27 May 1989. Using the red Air Schmidt camera with the 31.6 l/mm echelle, cross-disperser #3, the 200μm slit, and the GG495 order sorting filter, we obtained 17 km s⁻¹ spectral resolution from 5600 to 7000Å. We used decker 1 in April 1987 and decker 2 in 1989. The CCD detector was EPI #9 in 1987 and EPI #12 in 1989. We subtracted the overscan region and the CCD bias and trimmed the frames using IRAF. Subsequent reductions were undertaken using an echelle data reduction package written in IDL (Walter 1992). The data were flux-calibrated

using Kopff 27 and LTT 3864 as flux-standard stars. Most observations consisted of 3 sequential integrations; cosmic rays were filtered out by applying a median filter to the multiple observations of each target. The 1987 observations were compromised by unusually large flexure within the spectrograph. In some cases flexure shifted the spectra off the region illuminated by the projector flat (taken using decker 2), resulting in lower S/N than indicated by counting statistics alone. Radial velocities obtained during this run are unreliable, and have not been used.

We obtained multiple high-dispersion single-order spectra of each star with the echelle spectrographs of the Whipple Observatory 1.5-m reflector and the MMT between 1986 and 1993 for the purpose of measuring radial velocities. All the spectra were centered at $\lambda 5187\text{\AA}$ and provided about 50\AA coverage. Radial velocities were obtained via cross-correlation, following the procedures discussed by Nordstrom *et al.* (1994; see also Latham 1992). Cross-correlations were made against a grid of synthetic templates with a separation of 250K in temperature, 0.5 in $\log g$, and 10 km s^{-1} in $V \sin i$. For each star the radial velocity was adopted for that template providing the highest value for the average of the correlation peak. The typical precision of a single radial-velocity measurement is 1 km s^{-1} , based on the dispersions of repeated measurements. Rotational velocities were determined through an interpolation based on correlation peak strength, with a measurement lower limit of $\approx 10\text{ km s}^{-1}$. We estimate an uncertainty of 5 km s^{-1} .

UBVRI photometry was obtained in May 1986, June 1987, and May 1988 at CTIO. The data were obtained with the 1.0-m telescope using a Hamamatsu GaAs photomultiplier and apertures ranging from 15-20 arcseconds. All UBVR observations are on the Johnson (1963) system, while all R and I observations are on the Cousins (1980) system. We observed secondary standards from Landolt (1983). Additionally, a few UBVR observations were obtained for us by Dr. Robert Millis during May 1986 with the CTIO/Lowell 0.4-m telescope using an EMI6256 photomultiplier. Multiple, independent observations were obtained of each star during these observing runs with no obvious systematic differences in results between the various systems employed.

Further UBVRI photometry was obtained from CCD images acquired at CTIO on 1993 May 5 and 1994 June 3 using the 0.9 meter telescope. The detector used was the TEK 2K-1 CCD with the standard Bessell filter set. CCD debiasing and flat-fielding were performed using the IRAF CCDRED package. Instrumental magnitudes were determined using the IRAF APPHOT package. In the case of the close pair CrAPMS 6, photometry was performed on the individual stars after first subtracting off the other star using routines in the IRAF DAOPHOT package. The photometry was placed on the standard Johnson-Kron-Cousins system using calibration stars from Landolt (1992). Mean residual

errors are less than 3% except in the case of the CrAPMS 6 pair, which individually have mean residual errors of about 5%.

We also obtained near-infrared JHKL photometry during June 1986 using the CTIO 4-m telescope and during May 1989 using the CTIO 1.5-m telescope. Both observing runs employed a monolithic InSb detector and used standards from Elias *et al.* (1982) to place the observations onto the standard system. At the 4-m telescope a 6-arcsecond aperture was used, while at the 1.5-m telescope a 14-arcsecond aperture was used. One to five independent observations were obtained of each program star.

We obtained additional JHK observations on 19-21 February 1997, using the CIRIM imaging detector on the CTIO 1.5-m telescope. Each image consisted of a raster of 6 exposures, with the telescope offset by 15 arcsec between exposures. We observed standard stars from Elias *et al.* (1982). The non-linearity correction was applied using the IRAF task IRLINCOR. All subsequent data reductions were undertaken using IDL software written for the task. The images were flattened using dome-flats. The local sky was determined by median-filtering the six images, and was subtracted off. The frames were then registered and coadded. We used the standard star observations to determine the extinction correction for each night and place the photometry on the standard CIT system. Uncertainties in the photometric solution amount to ± 0.02 mag for single observations. Target fluxes were measured in an 8 arcsec radius aperture. For close binaries we measured the relative fluxes in smaller apertures, and then corrected to the total flux of the system.

3. The Optical Counterparts

We provide identifications for the low-mass stars following the IAU convention (Dickel *et al.* 1987) in Table 2. The identifications are the truncated J2000 coordinates. We also provide CrAPMS numbers which are shorter and easier to work with. Note that, by IAU convention, the proper designation for CrAPMS 1 is nTT J190134-3700. In this designation, the “nTT” prefix is retained for continuity with other papers in this series, and does not necessarily imply anything about the evolutionary status of the stars.

Finding charts for newly-identified stars are presented in Figure 2. A finding chart for CrAPMS 7 is given in Marraco & Rydgren (1981), and finding charts for CrAPMS 1, 2, and 3 are in Walter (1986). Optical spectra are shown in Figures 3 and 4. Low dispersion spectra of CrAPMS 1, 2, and 3 are in Walter (1986). Comments on the individual sources follow.

CrAPMS 1. This star has many aliases: CD -37° 13022, Anon 1 (Knacke *et al.* 1973),

i2 (Glass & Penston 1975), VSS13 (Vrba, Strom, & Strom 1976), CrA 1 (Walter 1986) and HBC 676 (Herbig & Bell 1988). Marraco & Rydgren (1981) noted weak Ca II H&K emission cores and 0.2 mag variability at V, and called it a PMS star with extremely weak emission.

CrAPMS 2. This is CD -37° 13029, a2 (Glass & Penston 1975), VSS1 (Vrba *et al.* 1976), CrA 2 (Walter 1986), and HBC 678 (Herbig & Bell 1988).

CrAPMS 3. This is star w (Glass & Penston 1975), VSS24 (Vrba *et al.* 1976), CrA 3 (Walter 1986), and HBC 679 (Herbig & Bell 1988). The faint optical companion visible to the northeast is very red, and is about 1.8 mag fainter than CrAPMS 3 at K ($J-K = 1.42 \pm 0.04$, $J-H = 1.00 \pm 0.04$).

CrAPMS 4. This source was found by running the MDETECT source-detection algorithm off-line. Two stars, designated 4NW and 4SE and separated by 43 arcsec, are within the X-ray error circle. Both are PMS stars.

CrAPMS 6. This 3 arcsec pair of M3 stars is H α 11 of Marraco & Rydgren. The stars appear of comparable brightness on the Palomar Observatory Sky Survey prints and on our CCD images, but on 3 dates (1987 June 5, 1988 May 24, and 1989 May 27) the SW component appeared faint. On 1988 May 24 the SW component was fainter than the NE component by 2.06 ± 0.48 magnitudes at V. In 1993 May the V magnitudes were identical within the errors. 6SW may be a large amplitude variable. 6NE is also variable, with a 0.3 mag range at V in 3 observations. In 1997 the K magnitudes were comparable.

CrAPMS 7. The counterpart is H α 6 of Marraco & Rydgren. H α 5 is on the edge of the 90% confidence error circle, but it is fainter, bluer, and does not have H α emission (Marraco & Rydgren 1981), and is unlikely to be PMS. H α 6 is a classical T Tauri star, with an infrared excess (Wilking *et al.* 1992) and a strong H α emission line ($W_\lambda(\text{H}\alpha) = -34\text{\AA}$).

CrAPMS 9. There are three stars in the 43 arcsec error circle. The star to the north is the PMS star; the close visual pair to the south shows neither evidence for H α emission nor Li absorption.

CrAPMS 10. This X-ray source is coincident with the pair of late-B stars HD 176269 (=HR7169 = SAO 210815) and HD 176270 (=HR7170 = SAO 210816). The resolution of the IPC is insufficient to split the pair.

CrAPMS 11. This source is coincident with the B9 star TY CrA, in the NGC 6726/7 nebulosity. TY CrA is a multiple system (e.g., Casey *et al.* 1993). The B9 star is part of a double-lined spectroscopic binary with a 2.9^d orbital period (Casey *et al.* 1995). The secondary is a $1.6 M_{\odot}$ G star. There is also a tertiary in the system.

We identified no spectroscopic binaries among the 6 stars observed at high dispersion. Four of the low-mass stars are in two visual pairs. We consider both to be physical pairs. The members of the wide CrAPMS 4 pair (~ 5000 AU projected separation) have essentially identical radial velocities, and the CrAPMS 6 pair consists of similar stars with a projected separation of 300 AU. The spatial association of each pair seems secure, but that they are gravitationally bound is not established, especially in the case of CrAPMS 4. Each of the higher mass objects, CrAPMS 10 and CrAPMS 11, are multiple. The binary fraction exceeds 56% (9 stars of 16 in multiple systems) or 36% (4 multiple systems of 11), depending on the definition. The binary fraction is higher (59% or 46%) if we assume that the companion to CrAPMS 3 is physical. The number of stars per system exceeds 1.4.

4. Discussion

4.1. The Low-Mass Stars

Seven of these 11 low-mass PMS stars were first noted through their X-ray emission, 5 here and 2 by Walter (1986); only the H α 11 pair (CrAPMS 6), H α 6 (CrAPMS 7), and Anon 1 (CrAPMS 1) were first identified using optical techniques. Once again, X-rays prove to be a powerful search technique for low-mass PMS stars.

The photometric magnitudes and colors are given in Tables 3 and 4. The second column of these tables gives the number of independent optical or near-infrared observations the listed photometry is based upon. Errors of a single observation in VRI were typically .01 mag at $V < 15$ mag, increasing to 0.03 mag at $V = 16$ mag, while at B and U the errors increased rapidly above 0.02 mag for $V > 14$, due to the red nature of these stars. However, the uncertainties in the optical photometry listed in Table 3 are dominated by the fact that all stars with sufficient numbers of observations showed evidence for variability. The range of observed variability is typically 0.15, 0.08, 0.04, and 0.02 mag for UBVR, respectively. For stars with many ($n \gtrsim 15$) observations, the variability appears consistent with rotational modulation by starspots with additional flaring visible in the U and B filters. In the near-IR, the uncertainties on a single observation are typically 0.02 mag (JHK) or 0.03 mag (L). Only CrAPMS 3 showed significant near-IR variability (Table 4); part or all of this may be attributable to its companion.

The measured radial (V_{rad}) and rotational ($V \sin i$) velocities and equivalent widths W_λ , the estimated spectral types and extinctions A_V , and the derived luminosities and masses are presented in Table 5. We determine the spectral types by visual comparison of the spectra with a grid of MK standards. We use the spectral types and the colors jointly to estimate the extinctions and luminosity classes. Temperatures are estimated from the unreddened R_C-I_C and $V-K$ colors (Laird 1985, Carney 1983, Veeder 1974), and agree with the spectral type temperature calibration of de Jager & Nieuwenhuijzen (1987), with a mean difference of 39K. For stars with $V-I_C > 1.57$, we use the color- T_{eff} calibration of Kirkpatrick *et al.* (1993). Stauffer (1997) has shown that this color- T_{eff} calibration brings the lower main sequence of the Pleiades into agreement with the D’Antona & Mazzitelli (1994) evolutionary tracks. Masses and ages are determined from the star’s location on the H-R diagram, and are dependent upon the choice of evolutionary track. Further details of the techniques may be found in Walter *et al.* (1994). We assume a distance of 130 pc to the association. On the basis of spatial association with the R CrA cloud, location above the main-sequence, luminosity classes, radial velocities, and the presence of Li I $\lambda 6707\text{\AA}$ absorption, all these stars are PMS. The dispersion in radial velocities is consistent with the 2 km s^{-1} velocity dispersion generally observed among PMS stars in the central parts of star-forming regions (Mathieu 1986).

The lithium abundances $\log N(\text{Li})$ (Table 5) are derived using the NLTE analysis of Pavlenko & Magazzù (1996). These curves of growth are valid for $T_{eff} > 3500\text{K}$; we extrapolate their curves of growth for our coolest stars ($3300\text{K} < T_{eff} < 3500\text{K}$). The abundances determined for the hotter stars are consistent with the abundances seen in T Tauri stars (Basri, Martin, & Bertout 1991). These are presumably the initial Li abundances, as depletion is not yet expected in stars of these masses. For the cooler stars, the abundances are seen to be significantly lower. Pre-main sequence lithium burning (e.g., Pinsonneault, Kawaler, & Demarque 1990) is expected among the M stars, but the expected depletion of less than half a dex for an age of $< 10 \text{ Myr}$ is significantly less than we measure. This discrepancy may be accounted for by the fact that the presence of an active chromosphere/transition region will over-ionize Li, giving an apparent underabundance (Houdebine & Doyle 1995). Note that the M stars with the largest $H\alpha$ equivalent widths have the smallest apparent Li abundances.

There is evidence of a near-IR excess attributable to warm circumstellar dust only in $H\alpha 6$ (CrAPMS 7).

X-ray count rates and derived luminosities, surface fluxes and flux ratios are given in Table 6. None of the targets were sufficiently bright to make extraction of the spectrum practical. We assume that the X-ray emission arises in a 10^7K corona for conversion to

luminosities and flux ratios. All derived quantities in Table 6 are corrected for extinction, assuming $R=3.1$. We divide the observed counts equally between the stars in the two pairs. This is a good assumption for CrAPMS 6, which consists of two similar stars, but probably not for the CrAPMS 4 pair. The luminosities and flux ratios are similar to those observed in other young associations (Walter *et al.* 1994).

The luminosity-temperature diagram for the X-ray-selected stars is presented in Figure 5. The two panels show the stars plotted against theoretical evolutionary tracks from D’Antona & Mazzitelli (1994), and from Swenson *et al.* (1994). The D’Antona & Mazzitelli tracks employ the Canuto & Mazzitelli (1990) treatment of convection and Alexander *et al.* (1989) opacities. Both sets of tracks are for solar abundances.

In the absence of other information, we must rely on the evolutionary tracks to estimate stellar masses and ages. We note the following in Figure 5:

1. The X-ray-selected stars are significantly older than the IR-excess stars discussed by Knacke *et al.* (1973) and by Wilking *et al.* (1992). Note that the X-ray and IR samples have few stars in common. Ages estimated from the Swenson *et al.* tracks are systematically older than those from the D’Antona & Mazzitelli tracks, by about a factor of 2. The mean ages are 7 and 15 Myr, relative to the D’Antona & Mazzitelli and the Swenson *et al.* tracks, respectively.
2. With the exception of CrAPMS 1, which appears significantly younger than the rest of the stars, the stars lie along a narrow locus.
3. There is no evidence that the $H\alpha$ -emitting stars $H\alpha$ 6 and $H\alpha$ 11 are significantly younger than the other X-ray-selected stars.

4.2. X-ray Emission from Higher Mass Stars

Two of the X-ray sources are coincident with late-B stars. TY Cra (B9V) is an eclipsing triple system (Casey *et al.* 1995). With a mass of $1.6 M_{\odot}$ and an age of <6 Myr, the secondary will be a G/K star similar to HDE283572 (Walter *et al.* 1987), and can easily account for all the observed X-ray flux. The tertiary mass is less certain: Casey *et al.* (1995) find $2.4 M_{\odot}$, while Corporon, Lagrange, & Beust (1996) find a mass of $1.2-1.4 M_{\odot}$. In either case the tertiary is likely to be an X-ray source. Both HR7169 (B9V) and HR7170 (B8IV-V), a 13 arcsec visual pair, are listed as spectroscopic binaries in the Yale Bright Star catalog (Hoffleit 1982); further observations are needed to determine if there are low-mass stars associated with the HR7169/70 system.

Are late-B stars in star-forming regions bright X-ray sources? A basic conclusion to be drawn from the EINSTEIN and ROSAT stellar X-ray observations is that all stars are X-ray sources — *except the late-B to mid-A stars*. Schmitt *et al.* (1993) observed the young Lindroos (1986) pairs, consisting of a near-zero-age main sequence B star and a young late-type visual companion. Using the ROSAT HRI, with 3 arcsec positional accuracy, they showed that in 4 cases *both* the B star and the late-type companion (ages less than 5×10^7 years) were X-ray sources. However, Caillault, Gagné, & Stauffer (1994) have argued that the fraction of late-B/early-A stars in the Orion Nebula which are detected as X-ray sources is just that fraction expected to have late-type (F5 or later) binary companions. Our data clearly do not help resolve the question of whether the late-B stars can be X-ray sources.

4.3. X-ray Emission from Classical T Tauri Stars

The classical T Tauri stars S CrA and DG CrA, and the intermediate-mass stars R CrA and T CrA were within the area viewed by the EINSTEIN observatory. None were detected. The 2σ upper limit to the IPC count rates is given in Table 7. The conversion from flux to counts depends on the assumed extinctions, which are poorly known. We assumed a coronal plasma at a temperature of 10^7 K. For a wide range of reasonable extinctions ($A_V \lesssim 10$ mag), the count rate limits correspond to coronal luminosities $L_X < 5 \times 10^{29}$ erg s^{-1} .

4.4. The Population of the R CrA Associations

Star formation in this cloud has been going on for a long time. The X-ray-selected stars, with ages extending upward to over 10 Myr, appear significantly older than the B stars and imbedded sources. The narrow locus occupied by the stars in the luminosity-temperature diagram may be evidence for a burst of star formation about 7-10 Myr ago, since younger stars will be more luminous, both at optical and X-ray wavelengths (that the imbedded IR sources are not detected is a consequence of their high extinction and the relatively high limiting flux in these short observations; Koyama *et al.* (1996) and Neuhäuser & Preibisch (1997), using ASCA and ROSAT, respectively, have reported the X-ray detection of imbedded class I protostars). However, given the small numbers, we cannot rule out continuous star formation at a constant rate over the last 10 Myr. Given this population of older stars, it appears that the R CrA cloud is not simply a lower mass analog of the ρ Oph cloud (Wilking *et al.* 1992), but may represent a more evolved state of such a cloud.

We observe 11 low-mass stars (counting visual pairs as 2 stars, and neglecting the

probable low-mass companions of the B stars) in these 9 X-ray error circles. In previous studies of the X-ray emitting populations of star-forming associations (Walter *et al.* 1988; 1994), we argued that the completeness of the X-ray sample is $\sim 30\%$. This incompleteness has been verified in the Taurus region by Neuhäuser *et al.* (1995). The same arguments hold here, implying that the total number of X-ray emitting low-mass PMS stars in the ~ 1.5 square-degrees observed is about 30. Therefore the total number of low-mass stars in this association must be about 60, or double that previously known.

This is an underestimate of the total population of the R CrA association. The X-ray observations sampled only about 1.5 square degrees near the center of the cloud. Over 10% (2 of 16) of those IR sources whose spectral energy distributions are consistent with their being PMS stars (Wilking *et al.* 1992 – see Figure 1) lie in the dark streamers to the east of the R CrA complex, near the B cloud (Rossano 1978) and outside the EINSTEIN IPC fields. If the X-ray sources are spatially distributed in the same way, the total number of X-ray emitting low-mass PMS stars must be increased by over 10%. Note that Neuhäuser *et al.* (1997) identified GSC 7916 0050, 1.6° to the southwest of R CrA and well outside the IPC fields, as a PMS star. In addition, some fraction of the X-ray bright population will lie behind the dark cloud, and will not be detected because their X-ray fluxes lie below our flux limit. Since 4 PMS systems are projected against the near side of the cloud, we would expect about the same number, or about 30% of the total population, to be hidden from view. These corrections would increase the inferred X-ray bright population (seen and unseen) to about 40 stars, and the total population to about 70 stars.

Wilking *et al.* (1994) claimed, based on IR source counts, that the total stellar population in the core 0.24 pc^2 of the CrA complex is small (~ 30 stars), assuming a 2 Myr age for the association. If the age is 10 Myr, their IR counts permit up to 78 association members in this small region (Wilking, private communication). Given the large uncertainties in the estimates and the differences in the volumes samples, there is no significant difference in the total population estimates from the IR or X-ray samples.

The X-ray-bright population is observed to be more widely dispersed in space than the IR-selected population. This is to be expected if the X-ray-bright population is older, and has some non-zero velocity dispersion. Some fraction of the total population may have dispersed outside the area we observed. To estimate the fraction of an old, dispersed population that should be visible within the volume sampled by the EINSTEIN observations, we modelled the association as a population with an age of 7 Myr and a velocity dispersion of 1.7 km s^{-1} , and neglect gravitational decelerations. We assume that the stars all form within 1° of the position of R CrA. If the star formation rate has remained constant over the past 7 Myr, then about 70% of the members of the association will lie

within the volume sampled. If the X-ray bright sample represents a short burst of star formation, with an age spread of 1 Myr, then only 45% of the population lies within the area sampled. Identifying the IR-bright sample with the youngest sources, and the X-ray bright sample with the non-imbedded older population, then the correction for the stars outside the IPC fields leads to an estimate of a total population of about 90 stars (in the case of continuous star formation, $N=70 \times 1.3$; in the case of 2 episodes of star formation, $N=30+40 \times 1.55$), with a likely uncertainty of ± 20 stars.

We are attempting to verify this estimate using an X-ray-selected sample of stars from observations with the ROSAT Observatory (Walter *et al.*, in preparation).

Wiling *et al.* (1992) noted that 25% of the stars in this association are of intermediate-mass (spectral types B8 to A5), an unusually large number. Other star formation regions (e.g., Upper Sco; Walter *et al.* 1994) show initial mass functions (IMF) similar to the field star mass function. If the R CrA IMF is consistent with the Miller-Scalo (1979) field star mass function, and the intermediate mass stars all have masses greater than $2.5 \pm 0.5 M_{\odot}$, then one expects a total population of 92_{-27}^{+34} stars with $M > 0.2 M_{\odot}$. Given the uncertainties in both the extrapolation of the IMF from 6 high mass stars and in our estimate of the low mass population, we see no evidence that the the mass function is abnormal. We conclude that the CrA clouds have spawned of order 100 low-mass stars over the past 10 Myr, and that there is no compelling evidence for an excess of intermediate-mass stars.

5. Summary

We have identified 11 low-mass pre-main-sequence X-ray emitting stars associated with the R CrA star-forming region. With the exception of H α 6, none of these stars have near-IR excesses attributable to warm circumstellar dust. None of the four classical T Tauri stars in the field were detected. X-ray emission was detected from the vicinity of the late-B stars TY CrA and HR 7169, but the emission may be attributable to lower mass companions.

Only 4 of the low-mass stars (2 in a close visual pair) were previously known from optical work to be PMS. The low-mass stars are significantly older than the 1-2 Myr age inferred for the infrared sources and intermediate-mass stars. The narrowness of the locus occupied by the X-ray-selected stars suggests an episode of star formation some 7 Myr ago, but we cannot exclude continuous star formation at a roughly constant rate over the past 10 Myr.

We estimate that the older nTT population dominates the total number of stars, and

that the total PMS population amounts to about 90 stars. Given 6 intermediate-mass stars, the number of low-mass stars is consistent (within the large uncertainties) with the field initial mass function.

This research has been supported by NSF grant AST89-96308, NASA grants NAG8-884, NAG5-1663 (ADP), and NAGW-1365 (Origins of Solar Systems) to SUNY, and NSF grant AST8814986 to the University of Wisconsin. RDM acknowledges support from the Presidential Young Investigator Program. The paper is based in part on observations collected at the European Southern Observatory, La Silla, Chile. We thank the folks at CfA, especially F. Seward and J. McSweeney, for their assistance with obtaining and examining the IPC images and using the measuring engine. We thank R. Millis for contributing a portion of the UBV photometry, and J. Stauffer for bringing to our attention an improved color- T_{eff} relation for M stars. We thank R. Davis, E. Horine, J. Peters, D. Latham, and A. Milone for assistance in the acquisition of the CfA radial velocity measurements, and Juan Alcalá of MPE Garching and the ESO staff at La Silla Observatory. This research made use of the SIMBAD database, operated by CDS, Strasbourg, France, and of the Digitized Sky Survey, produced at the Space Telescope Science Institute under grant NAGW-2166. We thank the referee for constructive criticisms and for bringing to our attention the near-IR brightness of the faint optical companion to CrPMS 3.

REFERENCES

- Alexander, D.R., Augason, G.C., & Johnson, H.R. 1989, ApJ, 345, 1014
- Barnes, J.V. & Hayes, D.S. 1982, IRS Standard Star Manual (AURA)
- Basri, G., Martin, E.L., & Bertout, C. 1991, A&A, 252, 625
- Caillault, J.-P., Gagné, M., & Stauffer, J.R. 1994, ApJ, 432, 386
- Canuto, V.M., and Mazzitelli, I. 1990, ApJ, 370, 295
- Carney, B.W. 1983. AJ, 88, 623
- Casey, B.W., Mathieu, R.D., Suntzeff, N.B., Lee, C., & Cardelli, J.A. 1993, AJ, 105, 2276
- Casey, B.W., Mathieu, R.D., Suntzeff, N.B., & Walter, F.M. 1995, AJ, 109, 2156
- Corporon, P., Lagrange, A.M., & Beust, H. 1996, A&A, 310, 228
- Cousins, A.W.J. 1980, S.Afr.Astron.Obs.Circ., 1, 234
- Cruddace, R.G. & Dupree A.K. 1984, ApJ, 277, 263
- D'Antona, F. & Mazzitelli, I. 1994, ApJS, 90, 467
- Dame, T.M., *et al.* 1987, ApJ, 322, 706
- de Jager, C. & Nieuwenhuijzen, H. 1987, A&A, 177, 217
- Dickel, H.R., Loret, M.-C., & de Boer, K.S. 1987, A&AS, 68, 75
- Elias, J.H., Frogel, J.A., Matthews, K., & Neugebauer, G. 1982, AJ, 87, 1029
- Feigelson, E.D. & Kriss, G.A. 1981, ApJL, 248, L35
- Feigelson, E.D., Casanova, S., Montmerle, T., & Guibert, J. 1993, ApJ, 416, 623
- Giacconi, R. *et al.* 1979, ApJ, 230, 540
- Glass, I.S. & Penston, M.V. 1975, MNRAS, 172, 227
- Herbig, G.H. & Bell, K.R. 1988, Third Catalog of Emission-Line Stars of the Orion Population, Lick Obs. Bull. No. 1111
- Hoffleit, D. 1982, *The Bright Star Catalogue*, 4th edition. (Yale University Observatory: New Haven)
- Houdebine, E.R. & Doyle, J.G. 1995, A&A, 302, 861
- Johnson, H.L. 1963, Basic Astronomical Data, edited by K. Aa. Strand, (Univ. of Chicago Press, Chicago), p. 204

- Kirkpatrick, J.D., Kelley, D.M., Rieke, G.H., Liebert, J., Allard, F., & Wehrse, R. 1993, *ApJ*, 402, 643
- Knacke, R.F., Strom, K.M., Strom, S.E., Young, E., & Kunkel, W. 1973, *ApJ*, 179, 847
- Koyama, K., Hamaguchi, K., Ueno, S., Kobayashi, N., & Feigelson, E.D. 1996, *PASJ*, 48, L87
- Kunkel, W.E. & Rydgren, A.E. 1979, *AJ*, 84, 633
- Laird, J.B. 1985, *ApJS*, 57, 389
- Landolt, A.U. 1983, *AJ*, 88, 439
- Landolt, A.U. 1992, *AJ*, 104, 340
- Latham, D.W. 1992, in *Complementary Approaches to Double and Multiple Star Research*, IAU Colloquium No. 135, ASP Conf. Series 32, edited by H.A. McAlister & W.I. Hartkopf, p. 110
- Lindroos, K.P. 1986, *A&A*, 156, 233
- Loren, R.B. 1979, *ApJ*, 227, 832
- Mathieu, R.D. 1986, in *Highlights of Astronomy*, edited by J.-P. Swings, p. 481
- Marraco, H.G. & Rydgren, A.E. 1981, *AJ*, 86, 62
- Miller, G.E. & Scalo, J.M. 1979, *ApJS*, 41, 513
- Montmerle, T., Koch-Miramond, L., Falgarone, E., & Grindlay, J.E. 1983, *ApJ*, 269, 182
- Mundt, R., Walter, F.M., Feigelson, E.D., Finkenzeller, U., Herbig, G.H., & Odell, A.P. 1983, *ApJ*, 269, 229
- Neuhäuser, R., Sterzik, M.F., Schmitt, J.H.M.M., Wichmann, R., & Krautter, J. 1995, *A&A*, 295, L5
- Neuhäuser, R., Thomas, H.-C., Danner, R., Peschke, S., & Walter, F.M. 1997, *A&A*, 318, L43
- Neuhäuser, R. & Preibisch, T. 1997, *A&A*, 322, L37
- Nordstrom, B., Latham, D.W., Morse, J.A., Milone, A.A.E., Kurucz, R.L., Andersen, J., & Stefanik, R.P. 1994, *A&A*, 287, 338
- Pavlenko, Y.V. & Magazzù, A. 1996, *A&A*, 311, 961
- Pinsonneault, M.H., Kawaler, S.D., & Demarque, P. 1990, *ApJS*, 74, 501
- Rossano, G.S. 1978, *AJ*, 83, 234

- Schmitt, J.H.M.M., Zinnecker, H., Cruddace, R., & Harnden, F.R., Jr., 1993, ApJL, 402, L13
- Stahler, S.W. 1988 ApJ, 293, 207
- Stauffer, J. 1997 in *Brown Dwarfs and Extrasolar Planets*, eds R. Rebolo, E.L. Martin, & M.R. Zapatero Osorio, ASP Conf. Series, in press
- Strom, K.M. & Strom, S.E. 1994, ApJ, 424, 237
- Swenson, F.J., Faulkner, J., Rogers, F.J., & Iglesias, C.A. 1994, ApJ, 425, 286
- Veeder, G.J. 1974, AJ, 79, 1056
- Vrba, F.J., Strom, S.E., & Strom, K.M. 1976, AJ, 81, 317
- Walter, F.M. 1986, ApJ, 306, 573
- Walter, F.M. 1992, AJ, 104, 758
- Walter, F.M., Brown, A., Mathieu, R.D., Myers, P.C., & Vrba, F.J. 1988, AJ, 96, 297
- Walter, F.M., Vrba, F.J., Mathieu, R.D., Brown, A., & Myers, P.C. 1994, AJ, 107, 692
- Walter, F.M., *et al.* 1987, ApJ, 314, 297
- Wilking, B., Giblin, T., McCaughrean, M., Rayner, J., Burton, M., & Zinnecker, H. 1994. in *Infrared Astronomy with Arrays: The Next Generation*
- Wilking, B.A., Greene, T.P., Lada, C.J., Meyer, M.R., & Young, E.T. 1992, ApJ, 397, 520

Fig. 1.— EINSTEIN Fields. The locations of the low-mass PMS stars are indicated by the filled circles. Open circles mark the B star systems TY CrA and HR 7169/70. Near-IR sources from compilation are marked by the ‘T’s.

Fig. 2.— Finding charts for the 6 newly-identified PMS stars. Each image is 4 arcmin on a side. These images are taken from the Digitized Sky Survey and have 1.7 arcsecond pixels. North is up and east is to the left.

Fig. 3.— Low-dispersion spectra. The data have been smoothed with a Fourier filter. The Y axis scale runs from zero to 120% of the maximum flux in the plotted interval. The prominent emission lines in the left panels are the chromospheric Ca II K&H lines. $H\alpha$ is the prominent emission line in the red spectra.

Fig. 4.— High-dispersion spectra. The discontinuities sometimes visible near 6465\AA and 6535\AA are the ends of the echelle orders. Plot scaling and smoothing are as in Figure 3. The left panel shows the $H\alpha$ emission line and a 150\AA stretch of continuum. A wide variety of $H\alpha$ line profiles is evident. The right panel shows the Li I ($\lambda 6707\text{\AA}$) and Ca I ($\lambda 6717\text{\AA}$) lines. Rotational broadening is evident in some spectra.

Fig. 5.— Two luminosity-temperature diagrams: one using the D’Antona & Mazzitelli (1994) evolutionary tracks; the other using the Swenson *et al.* (1994) tracks. Isochrones (dashed) are at ages of 1, 3, 6, 10, and 30 Myr; evolutionary tracks (dotted) are plotted for 0.2, 0.4, 0.5, 0.6, 0.7, 0.8, 0.9, 1.0, 1.2, 1.5, 1.8, and $2.0 M_{\odot}$. The birthline (Stahler 1988) and zero-age main sequence (Pinsonneault *et al.* 1990) are overplotted as solid lines for reference. Uncertainties in luminosity mainly indicate the uncertainty in the extinction correction.

Table 1. EINSTEIN IPC POINTINGS

Image	α (B1950)	δ (decimal degrees)	Time (sec)	Target
3501	283.849	-37.167	2128	ϵ CrA
4512	284.445	-37.016	2427	S CrA

Table 2. Positions of the CrA Stellar X-Ray Sources

nTT J	CrAPMS	GSC	α (J2000) δ		Other
185717-3643	4NW	7421 0665	18 57 17.8	-36 42 35.9	
185720-3643	4SE	7421 1242	18 57 20.7	-36 43 00.4	
185801-3655	5	7421 1040	18 58 01.7	-36 53 45.0	
185914-3711NE ^a	6NE		18 59 14.7	-37 11 30	H α 11
185914-3711SW	6SW		^b	^b	H α 11
190001-3637 ^c	7		19 00 01.5	-36 37 07	H α 6
190028-3656 ^a	8		19 00 28.9	-36 56 02	
190039-3648 ^a	9		19 00 39.1	-36 48 11	
—	10	7421 2294	19 01 03.1	-37 03 38.7	HR7169
—	”	7421 2295	19 01 04.2	-37 03 41.8	HR7170
190134-3700	1	7421 1890	19 01 34.9	-37 00 55.8	CrA 1 ^d
—	11	7421 1126	19 01 40.8	-36 52 36.3	TY CrA
190201-3707	2	7421 0493	19 02 01.9	-37 07 43.2	CrA 2 ^d
190222-3655	3	7421 1899	19 02 22.1	-36 55 40.8	CrA 3 ^d

^aCoordinates from Digitized Sky Survey, and represent the centroid of the light. These coordinates are not in the Guide Star frame.

^bThe SW component is 0.22^s west and 1.7” south of the NE component.

^cCoordinates from Marraco & Rydgren 1981.

^dWalter 1986.

Table 3. Visual Photometric Data

CrAPMS	n	V	ΔV	U-B	B-V	V- R_C	R_C-I_C
1	20	11.34	0.21	0.65	1.11	0.71	0.73
2	18	10.44	0.15	0.29	0.79	0.47	0.46
3	18	13.79	0.18	1.04	1.43	0.99	1.02
4NW	5	13.35	0.02	1.16	1.38	0.93	0.96
4SE	13	10.95	0.07	0.44	0.88	0.51	0.49
5	15	12.30	0.20	0.85	1.11	0.70	0.67
6NE	3	15.14	0.36	1.03	1.48	1.11	1.56
6SW ^a	1	15.34	0.96	1.26	1.82
7 ^b	1	13.93	1.26	0.85	1.00
8	3	15.68	0.14	1.20	1.47	1.30	1.66
9	1	15.88	...	1.47	1.65	1.26	1.58

^a The observed V magnitude was 17.14 ± 0.48 on 1988 May 24.

^bfrom Marraco & Rydgren (1981), and converted to the Cousins system using the transformation of Kunkel & Rydgren (1979).

Table 4. Near-IR Photometric Data

CrAPMS	n	K ^a	J-K	J-H	K-L
1	4	7.80	0.92	0.68	0.13
2	3	8.34	0.52	0.43	0.08
3 ^c	2	9.18	1.06	0.80	0.16
3 ^d	2	9.05	1.11	0.83	...
3 ^e	1	9.21	1.12	0.84	...
4NW	2	9.42	0.84	0.67	...
4SE	2	8.70	0.57	0.47	...
5	4	9.20	0.73	0.59	0.11
6NE	1	10.69	0.77	0.54	...
6NE	1	10.56	0.84	0.55	...
7 ^b	-	9.35	1.43	0.93	0.66
8	2	9.59	1.12	0.81	...

^aThe standard deviation of the mean is 0.02 mag for single observations, and 0.01 mag otherwise. Uncertainty on the colors is ± 0.04 mag for single observations, and ± 0.02 mag otherwise.

^b Data from Wilking *et al.* (1992).

^c Observations on 1986 June 2 and 3.

^d Observations on 1989 May 26 and 27.

^e Observations on 1997 February 21.

Table 5. Stellar Parameters

CrAPMS	Type	A_V^a	V_{rad}	V_{rot}	n^b	$W_\lambda(\text{Li})$	$\log N(\text{Li})^c$	$W_\lambda(\text{H}\alpha)$	T_{eff}	$\log (L/L_\odot)$	M/M_\odot^d
1	K1IV	1.2	-1.0	58	8	0.39	3.0	0.3	4702	0.19	1.0
2	G5IV	0.3	-1.2	23	20	0.28	3.1	-0.7	5281	0.10	1.2
3	K2IV	2.3	-1.2	<10	4	0.41	3.2	-0.9	4523	-0.31	0.9
4NW	M0.5V	0.2	-2.2	<10	5	0.45	2.0	-1.1	3886	-0.66	0.6
4SE	G5IV	0.5	-2.0	<10	6	0.36:	3.5	1.0	5302	-0.03	1.1
5	K5IV	0.1	-0.8	22	7	0.44	2.4	-0.8	4111	-0.51	0.7
6NE	M3V	0.2	-	0.70	2.2	-5.9	3525	-1.14	0.3
6SW	M3.5V	0.3	-	0.44	1.7	-9.8	3332	-1.06	0.2
7	M1V	0.6	-	0.36:	1.5	-33.5	3973	-0.66	0.7
8	M3V	1.6	-	0.57	2.1	-3.9	3631	-0.73	0.4
9	M2V	1.7	-	0.5:	1.9	-9.2	3704	-0.93	0.5

^aUncertainties typically ± 0.2 mag.

^bNumber of velocity observations.

^cLogarithmic Li abundances, interpolated from a grid by Pavlenko & Magazzù (1996) for $T_{eff} > 3500\text{K}$, and extrapolated for $T_{eff} < 3500\text{K}$. Uncertainties based on low dispersion spectra (equivalent widths followed by “:”) are roughly ± 0.3 dex.

^dMasses estimated from D’Antona & Mazzitelli (1994) tracks.

Table 6. X-Ray Fluxes

CrAPMS	$\text{c s}^{-1\text{a}}$	L_X^{b} ergs s^{-1}	F_X $\text{ergs cm}^{-2} \text{s}^{-1}$	$\frac{L_X}{L_{\text{bol}}}$
1	0.034 ± 0.005	2.9E30	1.4E7	4.5E-4
2	0.038 ± 0.006	2.2E30	1.8E7	4.0E-4
3	0.012 ± 0.003	1.7E30	1.5E7	7.2E-4
4NW ^c	0.014 ± 0.005	3.9E29	3.7E6	3.7E-4
4SE		4.6E29	5.1E6	1.1E-4
5	0.014 ± 0.005	6.3E29	8.9E6	5.2E-4
6NE ^c	0.011 ± 0.004	2.9E29	5.2E6	7.1E-4
6SW		3.1E29	3.7E6	7.3E-4
7	0.017 ± 0.004	1.1E30	2.9E7	1.1E-3
8	0.010 ± 0.003	9.6E29	9.2E6	1.1E-3
9	0.009 ± 0.003	8.9E29	1.4E7	1.5E-3

^aObserved count rate, broad band.

^bassuming emission from an equilibrium Raymond-Smith plasma at $\log T=7.0$.

^cCounts are divided equally between the two members of the pair.

Table 7. Upper Limits On Other YSOs

YSO	IPC Count Rate $\text{c s}^{-1} (2\sigma)$
R CrA	<0.004
S CrA	<0.004
T CrA	<0.003
DG CrA	<0.006

CrA

$-36^{\circ} 0^m$

$-36^{\circ} 30^m$

$-37^{\circ} 0^m$

δ

$-37^{\circ} 30^m$

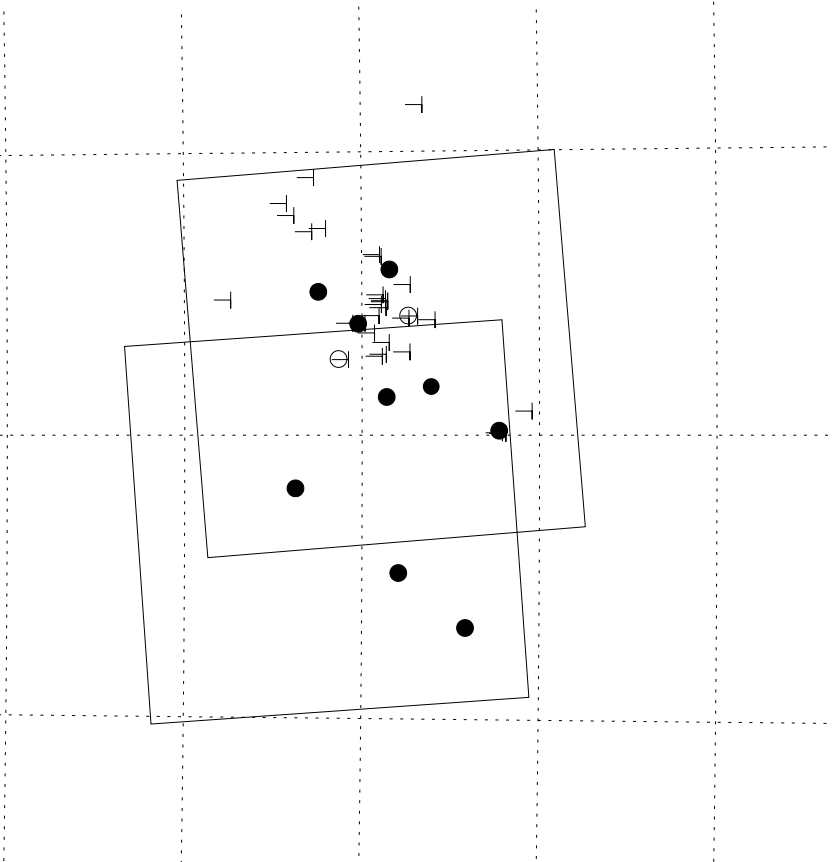
$-38^{\circ} 0^m$

$19^h 4^m$

$19^h 0^m$

$18^h 56^m$

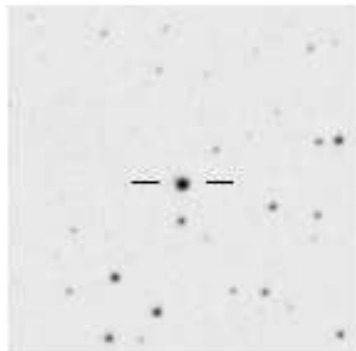
α (2000.0)



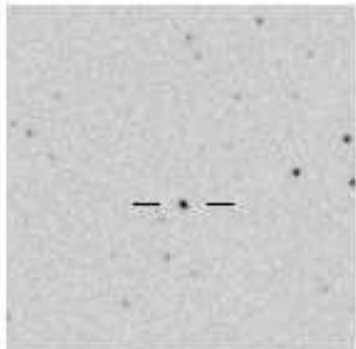
CrAPMS 4 NW/SE



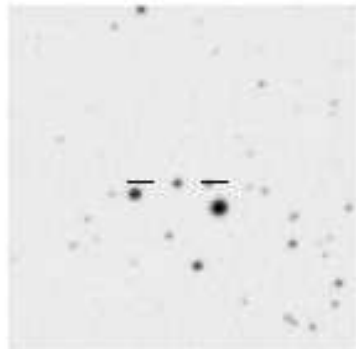
CrAPMS 5



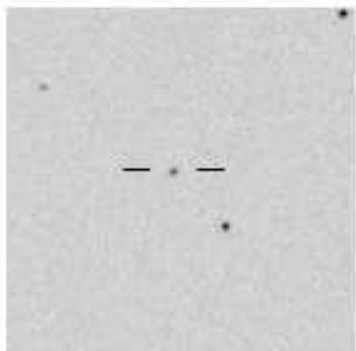
CrAPMS 6



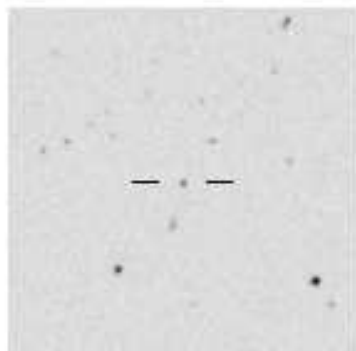
CrAPMS 7



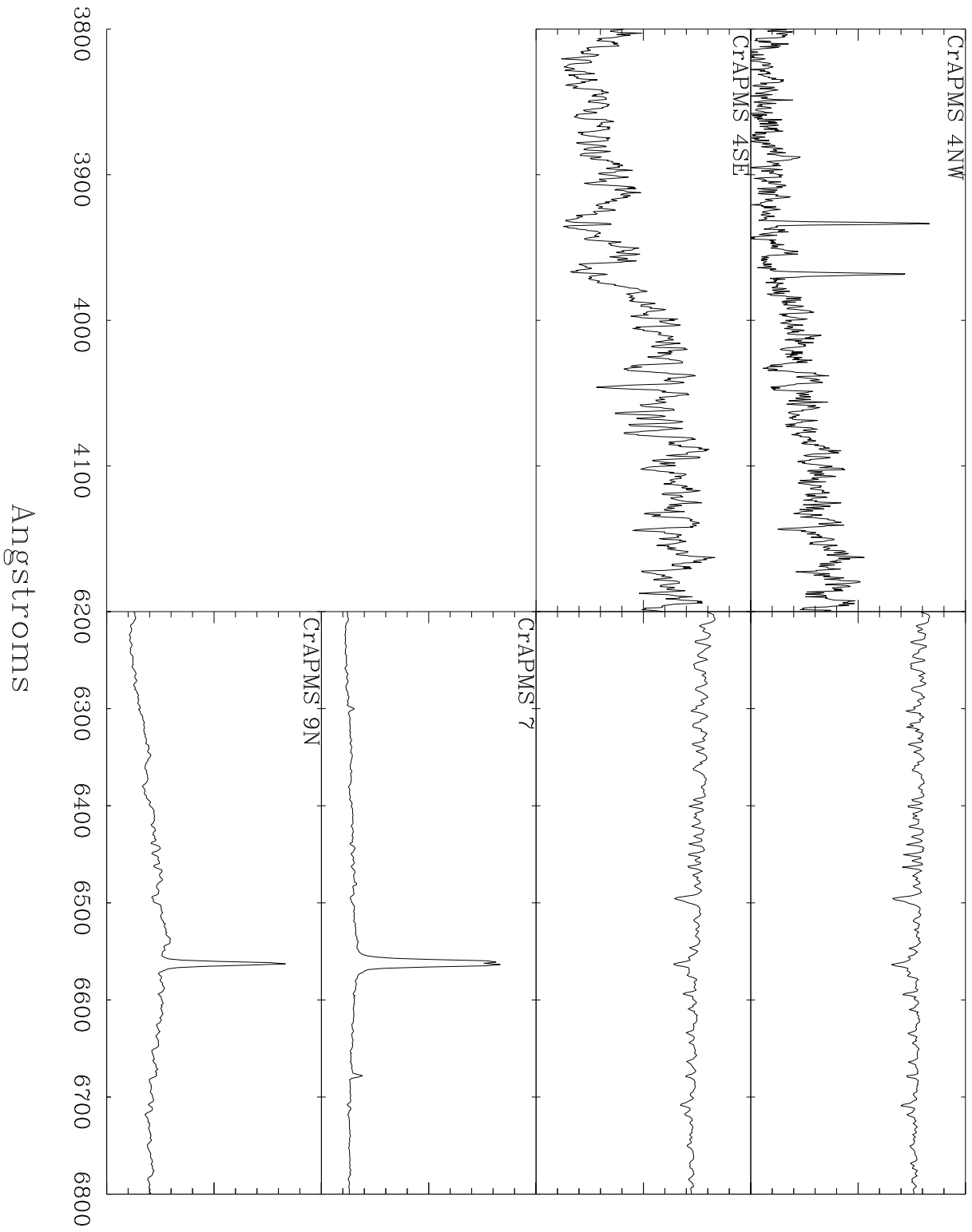
CrAPMS 8



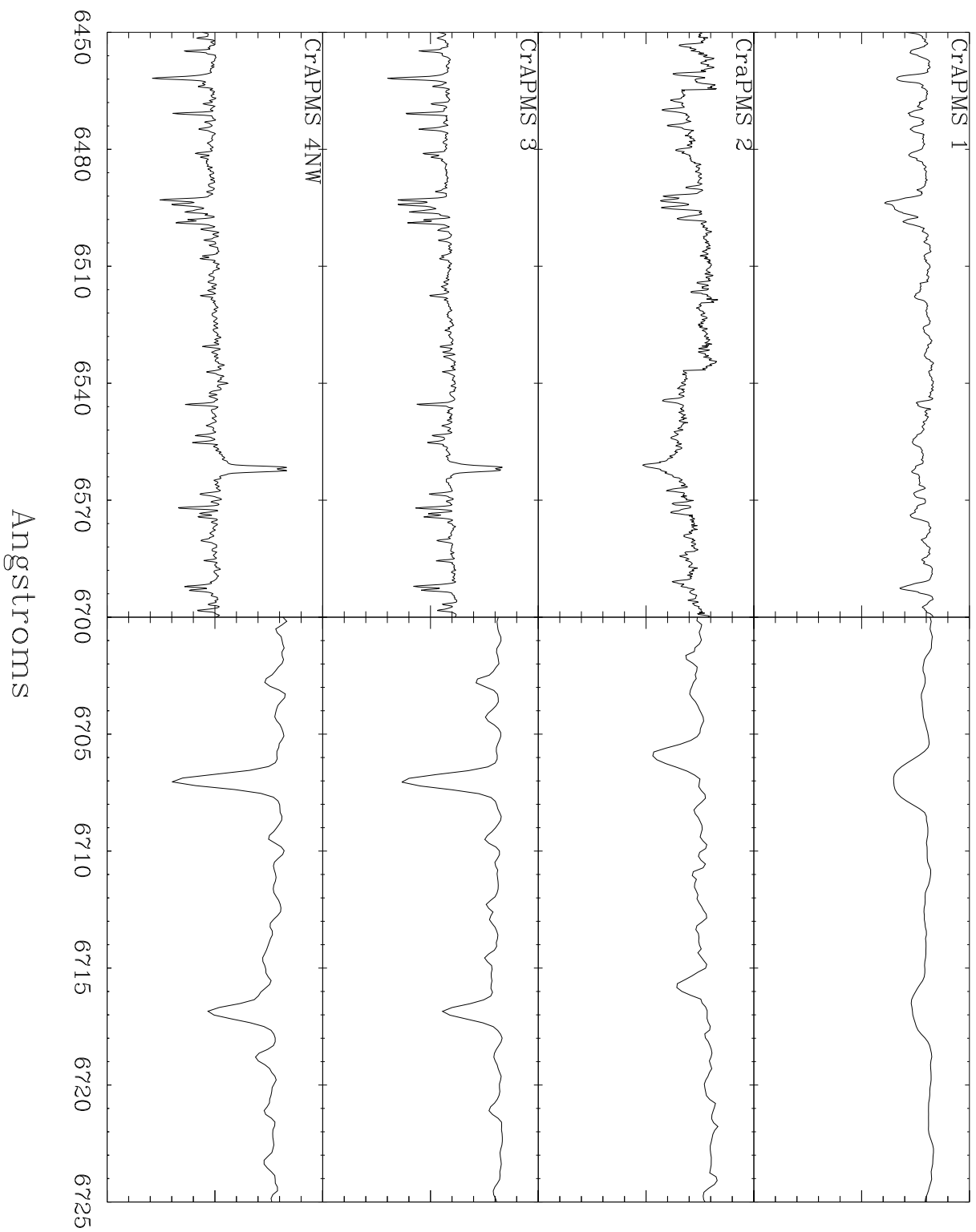
CrAPMS 9



F_λ (ergs cm⁻² s⁻¹ Å⁻¹)



F_λ (ergs cm⁻² s⁻¹ Å⁻¹)



F_{λ} (ergs cm⁻² s⁻¹ Å⁻¹)

